

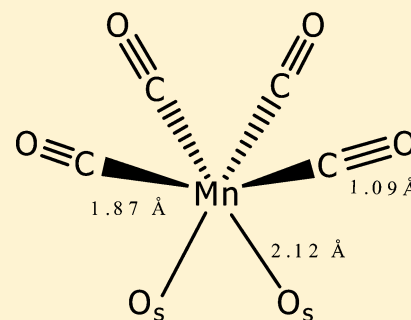
Formation of MgO-Supported Manganese Carbonyl Complexes by Chemisorption of $\text{Mn}(\text{CO})_5\text{CH}_3$

Supattra Khabuanchalad,^{†,‡} Jatuporn Wittayakun,^{*,†} Rodrigo J. Lobo-Lapidus,[‡] Stefan Stoll,[§] R. David Britt,[§] and Bruce C. Gates^{*,‡}

[†]School of Chemistry, Institute of Science, Suranaree University of Technology, Nakhon Ratchasima, Thailand 30000

[‡]Department of Chemical Engineering and Materials Science and [§]Department of Chemistry, University of California, Davis, California 95616, United States

ABSTRACT: MgO-supported manganese carbonyl complexes were prepared by chemical vapor deposition of $\text{Mn}(\text{CO})_5\text{CH}_3$ on partially dehydroxylated, high-area MgO powder. X-ray absorption spectra identify the resultant surface species, on average, as $\text{Mn}(\text{CO})_4(\text{O}_s)_2$ (where the two oxygen ligands are part of the MgO surface), and infrared spectra show that the chemisorption results from the reaction of $\text{Mn}(\text{CO})_5\text{CH}_3$ with OH groups of the MgO surface. Electron paramagnetic resonance and X-ray absorption near edge data indicate that the manganese was in a positive oxidation state other than +2, but the value is not determined, and the IR spectra indicate the presence of a mixture of manganese carbonyls. Extended X-ray absorption fine structure spectra determine the average Mn–CO bond distance to be 1.87 Å and the average Mn–O bond distance to be 2.12 Å. The surface complex was found to be stable in O_2 at room temperature.



INTRODUCTION

Supported transition metal catalysts, which are widely applied in technology, include many that are molecular analogues bonded to the surfaces of high-area porous metal oxides.^{1,2} The catalytic properties of a supported metal complex are influenced by the metal, its oxidation state and ligands, and the support, which itself is typically a ligand bonded to the metal by metal–oxygen bonds.³ The structures of supported metal complexes are usually determined spectroscopically, but interpretation of the spectra is often challenging because of the nonuniformity of the support surfaces and the species bonded to them.⁴ A set of complementary spectroscopic methods is usually required for a good structure determination, and interpretation of the spectra is challenging when the surface species are present in mixtures.

The synthesis of nearly uniform supported metal complexes is often optimized when the precursor is a molecular species with reactive ligands—typically, an organometallic complex.^{5,6} Metal carbonyl complexes are especially useful, because the CO ligands allow tracking of the surface chemistry by infrared (IR) and complementary spectroscopies. For example, the chemisorption of $\text{Fe}(\text{CO})_5$ on MgO leads to a mononuclear surface species represented as $[(\text{CO})_4\text{Fe}(\text{CO}_2)]^2\{\text{Mg}^{2+}\}$ (the braces represent groups on the support surface).⁷ Adsorption of $\text{H}_2\text{Os}(\text{CO})_4$ on MgO simply gives species represented as $\{\text{O}^{2-}\}\cdots\text{H}(\text{CO})_3\text{OsHCO}\cdots\{\text{Mg}^{2+}\}$.⁸ Adsorption of $\text{Re}(\text{CO})_5\text{H}$ on MgO results in surface species represented as an ion pair $[\text{Re}(\text{CO})_5]^- \cdots \text{H}^+\{\text{MgO}\}$.⁹ All of these metal carbonyls on surfaces were characterized by their ν_{CO} infrared (IR) spectra.

Beyond its value as a probe of structure of metal complexes, CO offers other advantages in investigations of supported metal catalysts: (a) CO is a weak electron-donor and a good π -

acceptor that stabilizes metal centers while being small enough to allow coordinative saturation of the complexes, (b) CO ligands are reactive intermediates in numerous catalytic reactions (such as CO oxidation and olefin hydroformylation), and (c) decarbonylation of supported metal carbonyls is sometimes possible under mild conditions, so that the surface species can be converted into metal complexes with a wide variety of ligands.^{10,11}

The chemistry of reactions of metal carbonyls with metal oxide surfaces is rich in complexity, including chemisorptions that are categorized as follows: those that involve (a) (partial) decarbonylation of the precursor,¹² (b) cleavage of metal–metal bonds,¹³ (c) adduct formation via bridging CO ligands,¹⁴ and (d) replacement of carbonyl ligands with other ligands,^{15–17} such as oxygen of the support surface. Furthermore, metal carbonyl cluster formation¹⁸ has been observed frequently on metal oxide surfaces, and it may be accompanied by or followed by fragmentation of the metal framework.¹⁹

The most widely investigated supported metal complexes are those of group-8 and group-9 metals, and only little has been reported for complexes of group-7 metals, almost all of them complexes of rhenium.^{15–17,20–22} Routes applied for the preparation of group-7 metal carbonyls on metal oxides include the reaction of $\text{Re}_2(\text{CO})_{10}$ with partially dehydroxylated MgO to give supported $[\text{Re}_2(\text{CO})_9]^{2-}$.²⁰ Treatment of these species in vacuum, helium, or air led to cluster fragmentation and the

Received: August 12, 2012

Revised: April 5, 2013

Published: April 24, 2013

formation of rhenium subcarbonyls identified as $[\text{Re}(\text{CO})_3\{\text{OMg}\}_x\{\text{HOMg}\}_{3-x}]$.²² The adsorption of $\text{H}_3\text{Re}_3(\text{CO})_{10}$ or of $\text{Re}(\text{CO})_5\text{H}$ on MgO involved breaking of Re–H bonds, giving $[\text{H}_2\text{Re}_3(\text{CO})_{12}]\{\text{MgO}\}$ or $\{\text{MgO}\}\text{H}^+\cdots[\text{Re}(\text{CO})_5]$, respectively. Treatment of each of these surface species in H_2 or helium gave mononuclear rhenium tricarbonyls.^{9,15,16}

Supported manganese complexes are represented by only a few reports,^{23,24} although they are of potential value because soluble manganese complexes are used as catalysts for oxidation reactions.^{25,26} There are several attractive manganese carbonyl precursors available for the preparation of supported complexes, including $\text{Mn}_2(\text{CO})_{10}$,^{27,28} $\text{Mn}(\text{CO})_5\text{H}$,²⁹ and $\text{Mn}(\text{CO})_5\text{Br}$.³⁰ In contrast to the adsorption of $\text{Re}_2(\text{CO})_{10}$, the adsorption of $\text{Mn}_2(\text{CO})_{10}$ on MgO produced a complex mixture of surface species, including physisorbed $\text{Mn}_2(\text{CO})_{10}$, manganese pentacarbonyl, and manganese tricarbonyl.²⁴ Characterization of the sample was complicated by the presence of a mixture of surface species, but when the sample was treated in O_2 , more nearly uniform surface species formed, represented as manganese tricarbonyl.²⁴

Thus, the surface chemistry of manganese complexes is related to that of rhenium complexes but is much more limited, and our goal was to extend this chemistry and develop a route to simple, nearly uniform manganese carbonyls. We chose a precursor with a high CO to Mn ratio, $\text{Mn}(\text{CO})_5\text{CH}_3$, and, for comparison with the work cited above,²⁴ MgO as the support. Because numerous manganese complexes are catalysts for oxidation reactions, the reactivity of the supported species with O_2 was also investigated.

$\text{Mn}(\text{CO})_5\text{CH}_3$ ³¹ is volatile, providing the opportunity to prepare supported samples by chemical vapor deposition (CVD)—that is, in the absence of solvents and the complications of solvent–support interactions. We set out to prepare supported species on MgO from $\text{Mn}(\text{CO})_5\text{CH}_3$ and to determine their structure by complementary spectroscopic methods, IR, electron paramagnetic resonance (EPR), and X-ray absorption spectroscopy (the latter including X-ray absorption near edge spectroscopy (XANES) and extended X-ray absorption fine structure (EXAFS) spectroscopy).

EXPERIMENTAL METHODS

Synthesis of $\text{Mn}(\text{CO})_5\text{CH}_3$. $\text{Mn}(\text{CO})_5\text{CH}_3$ was synthesized by a route analogous to that reported for $\text{Re}(\text{CO})_5\text{CH}_3$.³² The starting material was $\text{Mn}_2(\text{CO})_{10}$ (Strem, 98.0%) (instead of the $\text{Re}_2(\text{CO})_{10}$ used to prepare $\text{Re}(\text{CO})_5\text{CH}_3$). Mercury (Quicksilver Products, Inc.), sodium (Aldrich, 99%), anhydrous tetrahydrofuran (Aldrich, 99.9%), and methyl iodide (Acros Organics, 99%) were used without further purification. The synthesis and handling were performed with exclusion of air and moisture on a double-manifold Schlenk line.

The product $\text{Mn}(\text{CO})_5\text{CH}_3$, a white solid, was authenticated by its ¹H NMR³² (CD_2Cl_2) ($\delta = -0.09$ ppm) and IR spectra³³ ($\nu_{\text{CO}} = 2111(\text{w}), 2009(\text{vs}),$ and $1986(\text{w}) \text{ cm}^{-1}$).

Synthesis of MgO-Supported Sample from $\text{Mn}(\text{CO})_5\text{CH}_3$. MgO powder (EMD Science, 98.0%, BET surface area approximately $70 \text{ m}^2/\text{g}$) was calcined as described elsewhere.²⁴ In an N_2 -filled glovebox, a flask containing the $\text{Mn}(\text{CO})_5\text{CH}_3$ was quickly connected to another flask containing calcined MgO powder via a glass tube equipped with a high-vacuum valve. The apparatus was removed from the glovebox and connected to the Schlenk line. The flask containing $\text{Mn}(\text{CO})_5\text{CH}_3$ was placed in a dry ice/isopropanol bath. The system was evacuated for 15 min to remove N_2 , and then warmed to room temperature to allow sublimation of the $\text{Mn}(\text{CO})_5\text{CH}_3$ through the opened valve. The resultant solid sample formed by deposition of $\text{Mn}(\text{CO})_5\text{CH}_3$ on the MgO was evacuated overnight and stored in the

glovebox. The masses of $\text{Mn}(\text{CO})_5\text{CH}_3$ and MgO used in the synthesis were chosen to give a supported sample containing 1.0 wt % Mn prior to the evacuation step; during the evacuation step, any physisorbed $\text{Mn}(\text{CO})_5\text{CH}_3$ would have been removed from the sample by sublimation.

Treatment of Supported Samples. The sample was treated with O_2 in a once-through quartz tubular flow reactor at room temperature. The powder (1.0 g) was loaded into the reactor in the glovebox; it was held in place by a frit mounted near the center of the tube (the inside diameter was 1 cm), which was sealed on both ends by O-ring compression fittings. The reactor was removed from the glovebox, and then both ends were connected to the flow system—all without exposure of the sample to air. At room temperature, O_2 (0.1 bar) (Airgas, 10% by volume in helium) was fed continuously to the reactor at a rate of 60 mL (NTP)/min for 6 h, and then the sample was flushed with flowing helium, and the reactor was sealed and returned to the glovebox. The effluent gas from the reactor was analyzed periodically with an online mass spectrometer.

Spectroscopic Characterization of Samples. IR Spectroscopy. The partially dehydroxylated MgO and the sample prepared from $\text{Mn}(\text{CO})_5\text{CH}_3$ on MgO (before and after O_2 treatment) were characterized with a Bruker IFS 66v IR spectrometer equipped with DTGS and HgCdTe detectors. In the glovebox, each sample (0.1 g) was pressed between two KBr windows and placed in a gastight cell (International Crystal Laboratories, Garfield, NJ). The cell was then loaded into an airtight container. The container was removed from the glovebox and mounted in the spectrometer, and then the sample chamber was evacuated immediately (pressure ≈ 1 mbar), and the vacuum was maintained as spectra were recorded at room temperature, in transmission mode, with a resolution of 4 cm^{-1} . Each reported spectrum is the average of at least 128 scans.

X-ray Absorption Spectroscopy (XAS). The supported samples (before and after O_2 treatment) were characterized by XANES and EXAFS spectroscopies. Data were collected at beamline X-18B at the National Synchrotron Light Source (NSLS) at Brookhaven National Laboratory, Upton, NY. The beamline was equipped with a Si(111) double-crystal monochromator which was detuned by approximately 25–30% at the Mn K edge to minimize the effects of higher harmonics in the X-ray beam. The intensity of the X-rays entering and exiting the sample was measured with two gas-filled ion chambers, and a third ion chamber was used to collect the spectrum of a manganese foil used as a reference for energy calibration.

Each sample was loaded into a stainless-steel tube sealed with O-rings and transferred to the synchrotron, where it was handled in an N_2 -filled glovebox. The O_2 and moisture contents of the glovebox were less than 1.0 ppm. The mass of each sample (0.041 g) was calculated to provide an absorbance of about 2.5 to give a nearly optimized signal-to-noise ratio in the data.

The samples were weighed, mixed with inert boron nitride powder (Aldrich, 98.0%, particle diameter $\approx 1 \mu\text{m}$), packed into the cavity of a stainless-steel plate, and then sealed with Kapton tape. All the sample preparation steps were carried out in the glovebox to minimize the air exposure. The sample cell was transferred to the beamline and mounted between the first two ion chambers. Each sample was scanned at room temperature in transmission mode at the Mn K edge (6539 eV). Each reported spectrum is the average of at least four spectra.

EPR Spectroscopy. The calcined MgO and the supported samples before and after O_2 treatment were characterized by EPR spectroscopy. Each sample (0.05 g) in the N_2 -filled glovebox was loaded into a 4 mm O.D. quartz EPR tube and sealed with an Ultratorr fitting. The EPR tube was removed from the glovebox and evacuated (pressure $\approx 1 \times 10^{-3}$ mbar) for 30 min and then flame-sealed. EPR data were collected at the CalEPR Center at the University of California, Davis. Each sample was scanned at 50 K in a Bruker ECS 106 X-band spectrometer equipped with a Bruker ER4102ST cavity operating in the TE_{102} mode resonating at about 9.5 GHz. Measurements were performed with a microwave power of 10 mW, a field modulation of 0.2 mT at 100 kHz, and a sweep rate of 0.1 mT/s. Ten scans were accumulated for each reported spectrum.

XAS Data Analysis. EXAFS Data Analysis. EXAFS data analysis was conducted with a “difference file” technique³⁴ by use of the software XDAP.³⁵ The functions used to construct the structural models and minimize the error are shown elsewhere.³⁴ In the first step of the data analysis, all scans of a given sample were aligned and averaged. Reference backscattering amplitudes were calculated by using the FEFF7.0 software³⁶ from crystallographic data characterizing $\text{Mn}(\text{CO})_5\text{H}$ ³⁷ for representation of Mn–C and Mn–O_{CO} contributions (O_{CO} is carbonyl oxygen). The Mn–C–O moiety is characterized by colinear multiple scattering. $\text{Mn}_2(\text{CO})_{10}$ ²⁸ was used as a reference for Mn–Mn contributions, and Mn_2O_3 ³⁸ and MnMg alloy³⁸ were used as references for Mn–O_s (Mn–O_s refers to a relatively short Mn–O distance in supported samples incorporating oxygen of the support surface) and Mn–Mg contributions, respectively.

The data fitting was done in *R*-space (distance space) by using three *k*-weightings (k^0 , k^1 , and k^2). The candidate models accounted for all the plausible contributions, Mn–Mn, Mn–C, and Mn–O. For a candidate model to be considered appropriate, it was required to fit satisfactorily with all the *k*-weightings. In the fitting with each candidate model, the parameters characterizing each contribution (the coordination number *N*, the $\Delta\sigma^2$ value (disorder term), the interatomic distance *R*, and the inner potential correction ΔE_0) were varied until an optimized fit was obtained for all *k*-weightings. The number of parameters used in the fitting did not exceed the statistically justified number calculated with the Nyquist theorem.³⁹ The multiple scattering in $\text{Mn}_2(\text{CO})_{10}$ calculated with FEFF7.0 was used to identify and fit the colinear Mn–C–O contributions.

Two criteria⁴⁰ (besides the overall goodness of fit) were used to determine whether an EXAFS fit was satisfactory: first, analysis was done to determine whether the addition of each shell to the model improved the fit by decreasing the value of $(\Delta\chi)^2$, and, second, the parameters for each shell were checked to determine whether they were physically appropriate. Specifically, the value of ΔE_0 was constrained to be in the range –10 to 10 eV, and the magnitude of $\Delta\sigma^2$ was not to exceed $1.5 \times 10^{-2} \text{ \AA}^{-2}$.

XANES Data Analysis. Data in the XANES region were analyzed with the software package Athena.⁴¹ The edge position of the manganese in each sample was taken as the inflection point in the measured X-ray absorption spectrum. The energy scale of the spectrum was calibrated by setting the edge position of the manganese foil to the reported value.

RESULTS

Chemisorption of $\text{Mn}(\text{CO})_5\text{CH}_3$ on MgO. Observations during Synthesis. When the volatile white solid $\text{Mn}(\text{CO})_5\text{CH}_3$ was allowed to vaporize and come in contact with MgO powder by CVD, the color of the powder changed from white to pale yellow, indicating that the manganese complex adsorbed on the MgO.

Spectroscopic Characterization of Initially Prepared Sample. IR Spectroscopy: Spectra in the ν_{OH} Region. IR spectroscopy was used to characterize the OH groups on MgO and their reaction with the organomanganese precursor. The spectrum of the MgO before adsorption of the precursor (Figure 1, spectrum A) includes an intense band at 3765 cm^{-1} , attributed to singly coordinated OH groups (with the oxygen atom bonded to only one surface cation),⁴² as expected, and consistent with the inference that the support had been only partially dehydroxylated in the pretreatment. The IR spectrum of the sample incorporating the adsorbed manganese complex (Figure 1, spectrum B) shows a decrease in the intensity of the band assigned to the 1-coordinated OH groups on MgO, indicating that the precursor reacted with these groups.

Spectra in ν_{CH} and ν_{CO} Regions. IR bands corresponding to the CH_3 group (located at $2948(\text{w})$ and $2908(\text{w}) \text{ cm}^{-1}$ in the spectrum of the precursor $\text{Mn}(\text{CO})_5\text{CH}_3$) were not observed

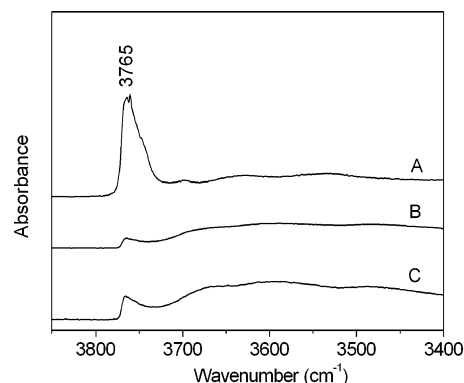


Figure 1. IR spectra in the ν_{OH} region of characterizing MgO (A), sample prepared by CVD of $\text{Mn}(\text{CO})_5\text{CH}_3$ on MgO (<1.0 wt % Mn) (B), and sample prepared by treatment of the sample represented by spectrum B in O_2 at 298 K and $P_{\text{O}_2} = 0.1$ bar (C).

in the spectrum of the supported sample, and so we infer that the CH_3 groups were removed from the manganese or otherwise converted as a result of the adsorption. The spectrum of the supported sample is characterized by ν_{CO} bands in positions different from those of $\text{Mn}(\text{CO})_5\text{CH}_3$ in CH_2Cl_2 solution (Figure 2, spectrum A) [$\nu_{\text{CO}} = 2012(\text{vs})$ and $1987(\text{m})$]

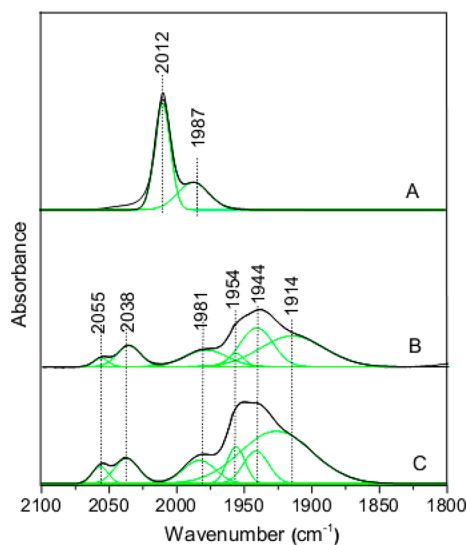


Figure 2. IR spectra of $\text{Mn}(\text{CO})_5\text{CH}_3$ in CH_2Cl_2 solution (A); of sample prepared by adsorption of $\text{Mn}(\text{CO})_5\text{CH}_3$ on MgO (<1.0 wt % Mn) (B); and of sample represented by spectrum B after O_2 treatment at 298 K and $P_{\text{O}_2} = 0.1$ bar (C). The peak deconvolutions are shown.

cm^{-1}], indicating that when the $\text{Mn}(\text{CO})_5\text{CH}_3$ reacted with MgO it was converted to other manganese carbonyl species. The spectrum of the supported sample (Figure 2, spectrum B) includes ν_{CO} bands at $2055(\text{w})$, $2038(\text{w})$, $1981(\text{w})$, and $1944(\text{s}) \text{ cm}^{-1}$. There are also shoulders at 1954 and 1914 cm^{-1} , with the frequencies having been determined by peak deconvolution. By comparison with the ν_{CO} IR spectra of known manganese carbonyl compounds (Table 1), we assign the spectrum of the supported species to a mixture of $\text{Mn}(\text{CO})_x$ species, including manganese tetracarbonyl complexes. After a few months, the spectrum of the supported species stored in the glovebox was essentially unchanged, demonstrating its stability.

Table 1. Manganese Carbonyl Compounds Incorporating Three or More Carbonyl Ligands and Supported Sample Prepared by Adsorption of Mn(CO)₅CH₃ on MgO

sample/compound	ν_{CO} (cm ⁻¹)	valence electrons on Mn determined by electron counting	ref
Mn ^I (CO) ₅ CH ₃ in CH ₂ Cl ₂	2012(vs) and 1987(m)	18	this work
Sample formed by CVD of Mn ^I (CO) ₅ CH ₃ on MgO	2055(w), 2038(w), 1981(w), 1954(sh,w), 1944(s), and 1914(sh,m)	18 ^a	this work
[Mn ^I (CO) ₄ Br] ₂	2056, 2023, 1982, 1954	16	43
[Mn(CO) ₄ P(OPh) ₃] ₂ Hg	2055, 2021, 1977, 1965, 1954	17	44
cis-[Mn ^I (CO) ₄ (P(OPh) ₃)CHO]	2070(w), 2000(sh, m), 1980(s), 1960(sh, m), (CHO)1590(m)	18	45
[Mn ^I (CO) ₄ (S ₂ PMe ₂)]	2086(w), 2015(vs), 1978(s), 1936(s)	18	46
[Mn ^I (CO) ₄ (S ₂ POMe ₂)]	2095(w), 2020(vs), 2003(s), 1965(s)	18	47
cis-[Mn ^I (CO) ₄ (PPh ₃)CHO]	2065(m), 1975(s), 1965(s), 1945(s), (CHO)1605(m)	18	45
[Mn ^I (CO) ₄ (tPr ₂ Me ₂)] ^b [BAR ₄ ^F] ^c	2077, 2000, 1980, 1971	18	48
[Mn ^I (CO) ₄ (tPr ₂ Me ₂)] ^b [BAR ₄ ^F] ^c	2077, 2000, 1980, 1971	18	48
Mn ^I (IPr)(CO) ₄ Br ^d	2078, 1995, 1938	18	48
Mn ^I (CO) ₅ CH ₃	2045(sh), 2023.6(vs), 2002(s,sh), 1961(w,sh) (gas phase)	18	49
[Mn ^I (CO) ₅ (PPh ₃)] [BF ₄]	2140(m), 2090(sh), 2070(sh), 2050(vs)	18	45
[Mn ^I (IPr)(CO) ₅][BAR ₄ ^F]	2134, 2049, 2045	18	48
[Mn(CO) ₆] ⁺	2090	18	50
[Mn ^I (CO) ₃ (tripod)] ^e [Mn(CO) ₅]	2030(s), 1962(s), 1902(ms), 1860(s)	18	23
Mn ^I (tPr ₂ Me ₂) ₂ (CO) ₃ Br	2004, 1926, 1864	16	48
{fac-Mn(CH ₃ CN)(CO) ₃ [H(pzAn ^{Me})] ^f }(PF ₆) (a manganese tricarbonyl with 3 nitrogen-containing ligands)	2052, 1956, 1919	18	51
fac-MnBr(CO) ₃ [H(pzAn ^{Me})]	major: 2029, 1936, 1913; minor: 2050, 1954	18	51
predominantly [Mn(CO) ₅] ⁻ on MgO (inferred to be ion paired with Mg ²⁺ sites)	2035, 1916, 1898, 1800	18	23,52
predominantly Mn(CO) ₃ (O _s) ₃ (sample formed from 1 wt % Mn ₂ (CO) ₁₀ on MgO after O ₂ treatment; O _s = oxygen of support surface)	2042(s), 1947(s), 1905(s)	16	24

^aSee text. ^btPr₂Me₂ = 1,3-diisopropyl-4,5-dimethylimidazol-2-ylidene. ^c[BAR₄^F] = B{C₆H₃(3,5-CF₃)₂}₄. ^dIPr = 1,3-bis(2,6-diisopropylphenyl)imidazol-2-ylidene. ^e(tripod) = 1,1,1-tris((diphenylphosphino)methyl)ethane. ^f[H(pzAn^{Me})] = 2-(pyrazolyl)-4-toluidine ligand.

The IR spectra suggest that a CO ligand was removed from Mn(CO)₅CH₃ upon adsorption, but these spectra alone are not sufficient to determine the structure of the supported species—because the manganese carbonyl compounds with spectra incorporating three or more ν_{CO} IR bands include tri-, tetra-, and pentacarbonyl complexes (Table 1).

EXAFS Spectroscopy. The EXAFS parameters representing this supported sample (Table 2) include Mn–C and Mn–O_{CO}

Table 2. EXAFS Parameters Characterizing Sample Prepared by Adsorption of Mn(CO)₅CH₃ on MgO^a

absorber–backscatterer pair	<i>N</i>	$\Delta\sigma^2 \times 10^{-3}$ (Å ²)	<i>R</i> (Å)	ΔE_0 (eV)
Mn–C	3.7	10.3	1.87	1.82
Mn–O _{CO}	3.8	7.10	2.96	1.82
Mn–O _s	2.2	9.37	2.12	8.34
Mn–Mg	1.2	2.05	3.48	9.71

^aNotation: *N*, coordination number; *R*, distance between absorber and backscatterer atoms; $\Delta\sigma^2$, sigma-squared value (disorder term); ΔE_0 , inner potential correction; O_{CO} oxygen of carbonyl group; O_{support} oxygen atom of MgO surface. In the fitting, the ΔE_0 values for Mn–C and Mn–O_{CO} contributions were constrained to be equal within error because the multiple scattering identified C and O atoms as present in linear Mn–C–O combinations (terminal manganese carbonyls). Typical accuracies are estimated to be as follows: *N*, ±20%; *R*, ±0.04 Å; $\Delta\sigma^2$, ±20%; ΔE_0 , ±20%.

contributions (O_{CO} is oxygen of carbonyl groups), each with a coordination number of approximately 4, showing that there were nearly four carbonyl ligands per Mn atom, on average; this result points to manganese tetracarbonyls as the average supported species.

The EXAFS data (Figure 3, Table 2) also indicate another Mn–O contribution, identified as Mn–O_{support} (where O_{support} refers to a surface oxygen atom of MgO) and a Mn–Mg contribution, with coordination numbers of approximately 2 and 1, respectively. The former was not characterized by colinear multiple scattering, confirming that it does not represent a Mn–O_{CO} contribution. The presence of the Mn–O_{support} contribution confirms that the manganese carbonyl precursor reacted with the MgO and identifies the support as a bidentate ligand in the average surface species. Consistent with this inference, the Mn–O_{support} distance of 2.12 Å is characteristic of bonding between manganese cations and oxygen ligands. For example, the distance between Mn²⁺ and O²⁻ in Mn/Co/TiO₂ characterized by EXAFS spectroscopy was reported to be 2.22 Å,⁵³ which matches the Mn–O distance of bulk MnO, determined crystallographically.⁵⁴ The role of the MgO support as a bidentate ligand matches that in presumably roughly analogous samples such as MgO-supported iridium complexes formed from Ir(C₂H₄)₂(acac)₅⁵⁵ and MgO-supported gold complexes formed from Au(CH₃)₂(acac).⁵⁶ The Mn–Mg contribution shows that the manganese complexes were

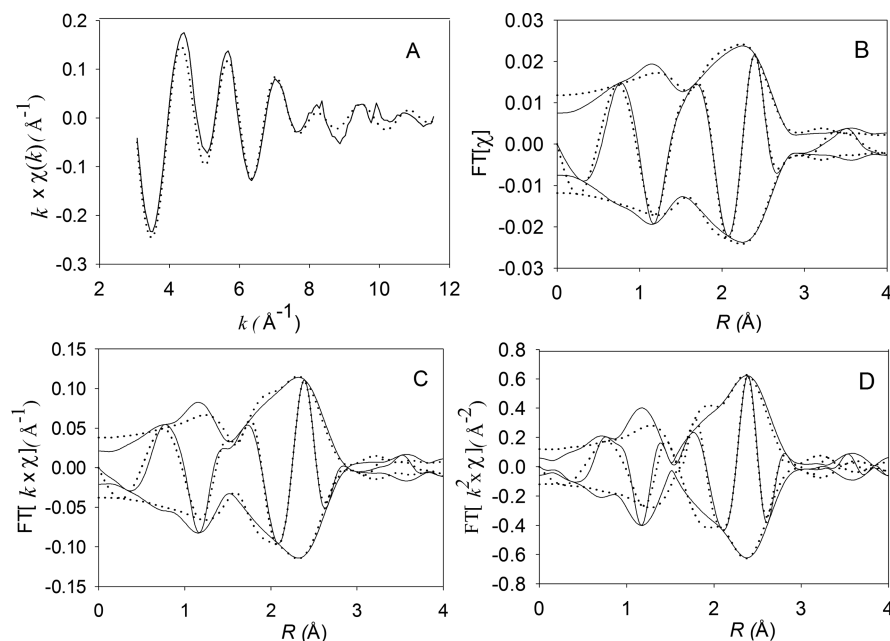


Figure 3. EXAFS data characterizing sample prepared by chemisorption of $\text{Mn}(\text{CO})_5\text{CH}_3$ on MgO (<1.0 wt % Mn) before O_2 treatment (—, data; ···, best-fit): k -weighted EXAFS function in k -space (A); imaginary part and magnitude of EXAFS function in R -space with Fourier transform (FT) k^0 -weighting (B), FT k^1 -weighting (C), and FT k^2 -weighting (D) ($\Delta k = 3.08\text{--}11.54 \text{ \AA}^{-1}$).

bonded to the MgO surface near Mg cations, and the lack of $\text{Mn}\text{--}\text{Mn}$ contributions confirms that the surface species remained mononuclear.

XANES Spectroscopy. The XANES spectrum characterizing the sample prepared from $\text{Mn}(\text{CO})_5\text{CH}_3$ and MgO is characterized by an edge energy of 6549 eV, which is 10 eV higher than that of manganese foil, indicating that the manganese was predominantly present as cationic species.

EPR Spectroscopy. The EPR spectrum of the calcined MgO (Figure 4) shows evidence of a CO_3^- radical on MgO .²⁴ This spectrum also includes a weak sextet ascribed to the hyperfine-split signal characterizing a small amount of divalent⁵⁵ Mn ($I = 5/2$) that is known to contaminate commercial MgO .²⁴ The EPR spectrum of the sample prepared from $\text{Mn}(\text{CO})_5\text{CH}_3$ and

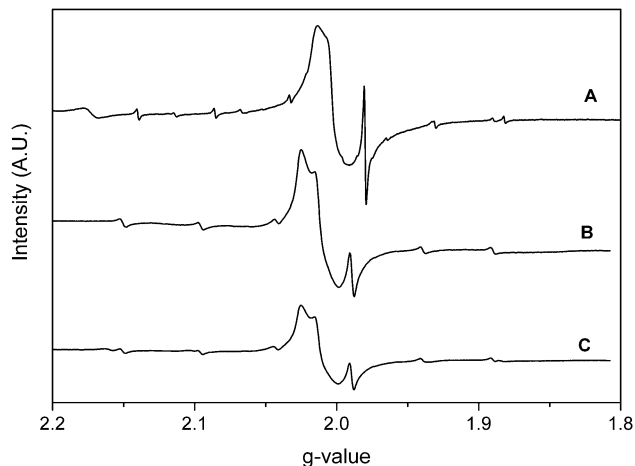


Figure 4. EPR spectra of pretreated MgO (A); sample prepared by adsorption of $\text{Mn}(\text{CO})_5\text{CH}_3$ on MgO (B), and sample prepared by adsorption of $\text{Mn}(\text{CO})_5\text{CH}_3$ on MgO after treatment in O_2 (C). Measurement conditions: temperature, 50 K; microwave power, 10 mW; modulation frequency, 100 kHz.

MgO shows no significant increase in the intensity of this contaminating Mn^{2+} signal (Figure 4, spectrum B). Six-coordinate Mn^{2+} complexes—a coordination number suggested for the Mn species formed on MgO (Table 1)—are typically characterized by a similar sextet signal.⁵⁷ Therefore, we conclude that the oxidation state of manganese in the supported species in this sample was not +2 and could have been either +1 (as in the precursor $\text{Mn}(\text{CO})_5(\text{CH}_3)$) and/or +3, as these species are EPR silent under standard X-band conditions. Because the EPR spectra of samples formed from $\text{Mn}(\text{CO})_5\text{CH}_3$ and MgO do not show new signals associated with manganese, any nascent paramagnetic species would have to have been present in low concentrations, to have an integer number of unpaired electrons (e.g., Mn^{3+}), or have oligomerized to yield EPR-silent species. This last possibility is not consistent with the EXAFS results, which give no evidence of $\text{Mn}\text{--}\text{Mn}$ contributions with a $\text{Mn}\text{--}\text{Mn}$ distance short enough to support such antiferromagnetic exchange.

Characterization of Samples after O_2 Treatment. **IR Spectroscopy.** The IR spectra in the ν_{OH} region of the sample prepared from $\text{Mn}(\text{CO})_5\text{CH}_3$ and MgO remained essentially unchanged after the sample was treated in O_2 at room temperature (Figure 1, spectrum C). This result shows that there was essentially no change in the OH groups on MgO as a result of the exposure to O_2 . The IR spectrum of this sample in the ν_{CO} region also includes no evidence of a significant change resulting from the O_2 treatment (Figure 2, spectrum C).

XANES Spectroscopy. The lack of any change in the edge energy of the sample prepared from $\text{Mn}(\text{CO})_5\text{CH}_3$ and MgO after the O_2 treatment indicates the lack of change in the electronic properties of the manganese in this sample during the O_2 treatment, consistent with the IR data.

Mass Spectra of Effluent Gas. The mass spectra characterizing the effluent gases flowing from the reactor during the O_2 treatment of the sample prepared from $\text{Mn}(\text{CO})_5\text{CH}_3$ and MgO do not show any evidence of CO , indicating that the CO ligands on manganese were not removed during the treatment.

Evidence of Manganese Oxidation State. A comparison of our XANES edge shifts with reported values of XANES calibration data characterizing manganese oxides (which are not consistent with each other)^{57–59} indicates that the manganese was cationic and that its oxidation state could have been as high as +5.^{57–59} Comparison of the XANES features characterizing the supported species with those of the XANES calibration samples indicate that the supported species are not analogues of those compounds. The EPR data rule out the value of +2, but otherwise the EPR and XANES data do not provide a sufficient basis for determining the manganese oxidation state. We address this point further in the Discussion.

Summary. The IR, XANES, and EPR spectra, combined with the mass spectrometric data, are all consistent with the stability of the supported manganese complexes prepared from $\text{Mn}(\text{CO})_5\text{CH}_3$ and MgO in O_2 at room temperature.

DISCUSSION

Chemisorption of $\text{Mn}(\text{CO})_5\text{CH}_3$ on MgO . The spectra characterizing the sample prepared from $\text{Mn}(\text{CO})_5\text{CH}_3$ and partially dehydroxylated MgO show that the chemisorption involved the reaction of the precursor with surface OH groups and the removal of CO and CH_3 ligands from the precursor. The EXAFS data show that the average supported species was manganese tetracarbonyl bonded to the MgO support by two Mn–O bonds. The initial manganese loading and the geometry of this average surface species indicated by the EXAFS data imply a coverage of the MgO of about 0.96 monolayers, but this value is an upper limit because any manganese carbonyl that was only physisorbed in the CVD process was removed by the subsequent overnight evacuation.

The XANES data are insufficient to determine the manganese oxidation state, beyond the statement that it is positive, and the EPR data rule out only the value of +2. The IR frequencies and their comparison with values characterizing carbonyl compounds of manganese in known oxidation states (Table 1) might be thought to provide additional information regarding the manganese oxidation state. These data characterizing the supported species are consistent with those of Mn^{I} compounds and, less likely, Mn^{III} compounds. Compounds in the latter class are not common, and so we infer that it is more likely that the predominant surface species was a Mn^{I} complex (although we do not rule out the possibility that it was a Mn^{III} complex or that minority Mn^{III} species were present).

Consistent with this suggestion, organomanganese complexes with manganese in the +1 oxidation state are commonly stabilized by π -acceptor ligands⁶⁰ (several examples are shown in Table 1). Assuming that the surface species was a Mn^{I} complex, we did the electron counting, considering surface oxygen ligands (like carbonyl ligands) to be two-electron donors. The results indicate that the surface species were 18-electron complexes, which are expected to be stable.

Because the EXAFS results indicate that the average surface species was a manganese tetracarbonyl, we suggest that the majority species might incorporate Mn^{I} with 18 valence electrons. The average Mn–C bond distance determined by EXAFS spectroscopy (1.87 Å, Table 2) agrees satisfactorily with the reported crystallographic data characterizing $[\text{Mn}^{\text{I}}(\text{CO})_4(\text{I}^{\text{Pr}}_2\text{Me}_2)_2][\text{BAr}_4^{\text{F}}]$ containing Mn^{I} , which incorporates two Mn–CO_{trans to CO} at 1.862 and 1.864 Å, and two Mn–CO_{trans to NHC} at 1.830 and 1.823 Å, but the symmetry arguments do not lead to the identification of a single manganese carbonyl compound that, on the basis of its IR

spectrum, is analogous to the surface manganese species. We infer that the surface manganese carbonyls were present in a mixture that we cannot resolve.

The shoulders in the IR spectra observed at 1954 and 1914 cm^{-1} characterizing the supported species formed from $\text{Mn}(\text{CO})_5\text{CH}_3$ and MgO and the sample formed by treatment of that supported sample in O_2 are suggested to be indications of minority surface species. The manganese complexes might have been bonded at various MgO surface sites (including defects), with different geometric arrangements of the support oxygen atoms as ligands, and there might have been hydrogen bonds between some of the carbonyl groups of the manganese complexes and surface hydroxyl groups of MgO , which would alter the frequencies of those groups. The data are consistent with such a hydrogen-bonded species.⁶¹ The minority species would not be expected to be detected by EXAFS spectroscopy, which does not provide such subtle details of the structure, especially when the species are minority species.

In the formation of the surface manganese species, the removal of OH groups from MgO and the removal of CH_3 groups from the precursor were both observed. The CH_3 groups might have reacted with OH groups to form CH_4 , as suggested by the work of Becker et al.,⁶² who investigated the amounts of gases liberated as helium flowed through samples made from $\text{Mn}(\text{CO})_5\text{CH}_3$ and dehydroxylated alumina (DA) and partially dehydroxylated alumina (PDA). Their results indicated that the CO removal from the sample prepared with PDA was significantly faster than when the support was DA. The liberation of CH_4 was observed when the sample was made from PDA but not when it was made from DA (a result that is attributed to the low OH content of the DA). Thus, on hydroxylated alumina, the protonolysis of the CH_3 ligand occurred during the adsorption of the precursor, resulting in CH_4 removal. By analogy, we infer that the same reaction likely occurred as $\text{Mn}(\text{CO})_5\text{CH}_3$ was chemisorbed on our MgO sample.

In our previous work, we prepared manganese complexes on the same support, using a similar synthesis procedure but a different precursor.²⁴ Deposition of $\text{Mn}_2(\text{CO})_{10}$ on MgO resulted in a sample with a complex IR spectrum indicating several surface species, and the characterization data indicate breaking of the Mn–Mn bonds as a result of the adsorption. After treatment in O_2 , a nearly uniform surface species, suggested by EXAFS spectra to be $\text{Mn}(\text{CO})_3(\text{O}_{\text{support}})_3$, was obtained; decarbonylation took place during treatment of the sample with O_2 . In the present work, deposition of $\text{Mn}(\text{CO})_5\text{CH}_3$ resulted in a mixture of surface species that are relatively stable in O_2 and are characterized by a higher CO to Mn ratio than was formed by the aforementioned sample represented as $\text{Mn}(\text{CO})_3(\text{O}_s)_3$. The comparison shows that by changing the manganese precursor one can prepare different manganese surface species with different numbers of carbonyl ligands. The stability of our new surface species in O_2 might suggest their stability under conditions of catalytic oxidation.

CONCLUSIONS

The reaction of $\text{Mn}(\text{CO})_5\text{CH}_3$ with the surface OH groups of partially dehydroxylated MgO led to the formation of supported manganese carbonyl species, which EXAFS spectra show, on average, to be $\text{Mn}(\text{CO})_4(\text{O}_s)_2$, where the two oxygen ligands are part of the MgO surface. The average bond distances determined by EXAFS spectroscopy are the following: Mn–C, 1.87 Å; Mn–O_{support}, 2.12 Å; and C–O,

1.09 Å. IR spectra show that a mixture of manganese carbonyls formed. The supported cationic manganese species were found to be stable in O₂ at room temperature.

AUTHOR INFORMATION

Corresponding Author

*E-mail: jatuporn@sut.ac.th (J.W.); bcgates@ucdavis.edu (B.C.G.).

Notes

The authors declare no competing financial interest.

ACKNOWLEDGMENTS

We thank T. A. Stich for helpful comments and an anonymous reviewer for insightful comments that led to an improved interpretation of the IR spectra. S.K. is grateful for support from the program Strategic Scholarships for Frontier Research Network from the Office of the Higher Education Commission, Thailand. This research was supported by the U.S. Department of Energy (DOE), Office of Energy Research, Basic Energy Sciences, Grant Numbers DE-FG02-04ER15513 and FG02-87ER15600 (R.J.L.-L.). We acknowledge beam time and the support of DOE, Office of Science, Materials Sciences, for its role in the operation and development of beamline X-18B of the National Synchrotron Light Source. We acknowledge the CalEPR Center at UC Davis for access to the EPR instrument.

REFERENCES

- Hlatky, G. G. Heterogeneous Single-Site Catalysts for Olefin Polymerization. *Chem. Rev.* **2000**, *100*, 1347–1376.
- Yoneda, N.; Kusano, S.; Yasui, M.; Pujado, P.; Wilcher, S. Recent Advances in Processes and Catalysts for the Production of Acetic Acid. *Appl. Catal., A* **2001**, *221*, 253–256.
- Basset, J.-M.; Psaro, R.; Roberto, D.; Ugo, R., Eds. *Modern Surface Organometallic Chemistry*; Wiley-VCH: Weinheim, Germany, 2009.
- Schneider, R. L.; Howe, R. F.; Watters, K. L. Interaction of Cobalt Carbonyls with Oxide Surfaces. 3. Dicobalt Octacarbonyl and Tetracobalt Dodecacarbonyl in Zeolites. *Inorg. Chem.* **1984**, *23*, 4600–4607.
- Chotisuwan, S.; Wittayakun, J.; Gates, B. C. Pt₃Ru₆ Clusters Supported on γ -Al₂O₃: Synthesis from Pt₃Ru₆(CO)₂₁(μ_3 -H)(μ -H)₃, Structural Characterization, and Catalysis of Ethylene Hydrogenation and *n*-Butane Hydrogenolysis. *J. Phys. Chem. B* **2006**, *110*, 12459–12469.
- Psaro, R.; Recchia, S. Supported Metals Derived from Organometallics. *Catal. Today* **1998**, *41*, 139–147.
- Guglielminotti, E.; Zecchina, A. Spectroscopic Study of the Adsorption and Vacuum Decarbonylation of Fe(CO)₅ on MgO. *J. Mol. Catal.* **1984**, *24*, 331–344.
- Lamb, H. H.; Gates, B. C. Molecular Organosmium Chemistry and Catalysis on the Basic Magnesium Oxide Surface. *J. Am. Chem. Soc.* **1986**, *108*, 81–89.
- Kirlin, P. S.; van Zon, F. M. B.; Koningsberger, D. C.; Gates, B. C. Surface Catalytic Sites Prepared from [HRe(CO)₅] and [H₃Re₃(CO)₁₂]: Mononuclear, Trinuclear, and Metallic Rhenium Catalysts Supported on MgO. *J. Phys. Chem.* **1990**, *94*, 8439–8450.
- Fierro-Gonzalez, J. C.; Kuba, S.; Hao, Y.; Gates, B. C. Oxide- and Zeolite-Supported Molecular Metal Complexes and Clusters: Physical Characterization and Determination of Structure, Bonding, and Metal Oxidation State. *J. Phys. Chem. B* **2006**, *110*, 13326–13351.
- Liang, A. J.; Craciun, R.; Chen, M.; Kelly, T. G.; Kletniaks, P. W.; Haw, J. F.; Dixon, D. A.; Gates, B. C. Zeolite-Supported Organorhodium Fragments: Essentially Molecular Surface Chemistry Elucidated with Spectroscopy and Theory. *J. Am. Chem. Soc.* **2009**, *131*, 8460–8473.
- Hugues, F.; Basset, J.-M.; ben Taarit, Y.; Choplin, A.; Primet, M.; Rojas, D.; Smith, A. K. Surface organometallic chemistry: formation of HFe₃(CO)₁₁⁻ from Fe₃(CO)₁₂ and Fe(CO)₅ on silica, alumina, magnesia, and zinc oxide. *J. Am. Chem. Soc.* **1982**, *104*, 7020–7024.
- Purnell, S. K.; Xu, X.; Goodman, D. W.; Gates, B. C. Adsorption and Reaction of [Re₂(CO)₁₀] on Ultrathin MgO Films Grown on a Mo(110) Surface: Characterization by Infrared Reflection-Absorption Spectroscopy and Temperature-Programmed Desorption. *J. Phys. Chem.* **1994**, *98*, 4076–4082.
- Youngs, C. T.; Correa, F.; Ploch, D.; Burwell, R. L.; Shriver, D. F., Jr. Chemistry of the Interaction of some Metal Carbonyl Clusters with Metal Oxide Surfaces. [CpFe(CO)]₄, Cp₃Ni₃(CO)₂, and [CpNi(CO)]₂ on Alumina. *Organometallics* **1983**, *2*, 898–903.
- Kirlin, P. S.; Knözinger, H.; Gates, B. C. Mononuclear, Trinuclear, and Metallic Rhenium Catalysts Supported on MgO: Effects of Structure on Catalyst Performance. *J. Phys. Chem.* **1990**, *94*, 8451–8456.
- Kirlin, P. S.; DeThomas, F. A.; Bailey, J. W.; Gold, H. S.; Dybowski, C.; Gates, B. C. Molecular Oxide-supported Rhenium Carbonyl Complexes: Synthesis and Characterization by Vibrational Spectroscopy. *J. Phys. Chem.* **1986**, *90*, 4882–4887.
- Lobo-Lapidus, R. J.; Gates, B. C. Supported Rhenium Complexes: Almost Uniform Rhenium Tricarbonyls Synthesized from CH₃Re(CO)₅ and HY Zeolite. *Langmuir* **2010**, *26*, 16368–16374.
- Kulkarni, A.; Mehraeen, S.; Reed, B. W.; Okamoto, N. L.; Browning, N. D.; Gates, B. C. Nearly Uniform Decaosmium Clusters Supported on MgO: Characterization by X-ray Absorption Spectroscopy and Scanning Transmission Electron Microscopy. *J. Phys. Chem. C* **2009**, *113*, 13377–13385.
- Bhirud, V. A.; Iddir, H.; Browning, N. D.; Gates, B. C. Intact and Fragmented Triosmium Clusters on MgO: Characterization by X-ray Absorption Spectroscopy and High-resolution Transmission Electron Microscopy. *J. Phys. Chem. B* **2005**, *109*, 12738–12741.
- Papile, C. J.; Knözinger, H.; Gates, B. C. [Re₂(CO)₉]²⁻ on Hydroxylated MgO: Formation from [Re₂(CO)₁₀] and Evidence of Ion Pairing at the Surface. *Langmuir* **2000**, *16*, 5661–5664.
- Kirlin, P. S.; Gates, B. C. Activation of the C–C Bond provides a Molecular Basis for Structure Sensitivity in Metal Catalysis. *Nature* **1987**, *325*, 38–39.
- Papile, C. J.; Gates, B. C. Rhenium Subcarbonyls on Magnesium Oxide: Identification of the Surface Oxo and Hydroxo Ligands by Infrared Spectroscopy. *Langmuir* **1992**, *8*, 74–79.
- Keyes, M. P.; Gron, L. U.; Watters, K. L. Interactions of Nickel and Manganese Carbonyls with Oxide Surfaces—Formation of Reduced, Oxidized, and Zerovalent Metal Species. *Inorg. Chem.* **1989**, *28*, 1236–1242.
- Khabuanchalad, S.; Wittayakun, J.; Lobo-Lapidus, R. J.; Stoll, S.; Britt, R. D.; Gates, B. C. Formation of a Manganese Tricarbonyl on the MgO Surface from Mn₂(CO)₁₀: Characterization by Infrared, Electron Paramagnetic Resonance, and X-ray Absorption Spectroscopies. *J. Phys. Chem. C* **2010**, *114*, 17212–17221.
- Ishii, H.; Ueda, M.; Takeuchi, K.; Asai, M. J. Oxidative Carbonylation of Phenol to Diphenyl Carbonate Catalyzed by Pd₂Sn Heterotrimeric Complex along with Mn Redox Catalyst without any Addition of Ammonium Halide. *J. Mol. Catal. A Chem.* **1999**, *144*, 369–372.
- Tagliatesta, P.; Giovannetti, D.; Leoni, A.; Neves, M. G. P. M. S.; Cavaleiro, J. A. S. Manganese(III) Porphyrins as Catalysts for the Oxidation of Aromatic Substrates: An Insight into the Reaction Mechanism and the Role of the Cocatalyst. *J. Mol. Catal. A: Chem.* **2006**, *252*, 96–102.
- Ramallo-López, J. M.; Lede, E. J.; Requejo, F. G.; Rodriguez, J. A.; Kim, J. Y.; Rosas-Salas, R.; Domínguez, J. M. XANES Characterization of Extremely Nanosized Metal-carbonyl Subspecies (Me = Cr, Mn, Fe, and Co) Confined into the Mesopores of MCM-41 Materials. *J. Phys. Chem. B* **2004**, *108*, 20005–20010.
- Dahl, L. F.; Rundle, R. E. Crystal Structure of Dimanganese Decacarbonyl, Mn₂(CO)₁₀. *Acta Crystallogr.* **1963**, *16*, 419–427.

- (29) Edgell, W. F.; Fisher, J. W.; Asato, G.; Risek, W. M. Infrared Spectrum and Vibrational Assignments for Pentacarbonylmanganese Hydride. *Inorg. Chem.* **1969**, *8*, 1103–1108.
- (30) Huang, Y.; Poissant, R. R.; Qiu, P. Study of the Reactivity of $\text{Mn}(\text{CO})_5\text{Br}$ on the Surface of Zeolites by Fourier Transform Raman and Infrared spectroscopy. *Langmuir* **2000**, *16*, 889–893.
- (31) Urbancic, M. A.; Shapley, J. R.; Sauer, N. N.; Angelici, R. J. Pentacarbonylhydridorhenium. In *Inorganic Syntheses*; Kaesz, H. D., Ed.; Wiley: Hoboken, NJ, 1989; Vol. 26, pp 77–80.
- (32) Zybilla, C. E. *Synthetic Methods of Organometallic and Inorganic Chemistry*; Georg Thieme Verlag: New York, 1997.
- (33) Mahmood, Z.; Azam, M.; Mushtaq, A.; Kausar, R.; Kausar, Gilani, S. R. Comparative Vapour phase FTIR Spectra and Vibrational Assignment of Manganese Pentacarbonyls Derivatives of the Type $\text{XMn}(\text{CO})_5$; (where X = Br, Cl, I, H, D, CH_3 , CD_3 , CF_3). *Spectrochim. Acta A* **2006**, *65A*, 445–452.
- (34) Koningsberger, D. C.; Mojet, B. L.; van Dorssen, G. E.; Ramaker, D. E. An atomic X-ray Absorption Fine Structure Study of the Influence of Hydrogen Chemisorption and Support on the Electronic Structure of Supported Pt Particles. *Top. Catal.* **2000**, *10*, 157–165.
- (35) Vaarkamp, M.; Linders, J. C.; Koningsberger, D. C. A New Method for Parameterization of Phase Shift and Backscattering Amplitude. *Phys. B* **1995**, *209*, 159–160.
- (36) Rehr, J. J.; Albers, R. C. Theoretical Approaches to X-ray Absorption Fine Structure. *Rev. Mod. Phys.* **2000**, *72*, 621–656.
- (37) La Placa, S. J.; Hamilton, W. C.; Ibers, J. A. Crystal and Molecular Structure of Manganese Pentacarbonyl Hydride. *Inorg. Chem.* **1964**, *3*, 1491–1495.
- (38) Pearson, W. B.; Calvert, L. D.; Villars, P. *Pearson's Handbook of Crystallographic Data for Intermetallic Phases*; American Society for Metals: Metals Park, OH, 1985.
- (39) Sayers, D. E.; Stern, E. A.; Lytle, F. W. New Technique for Investigating Noncrystalline Structures: Fourier Analysis of the Extended X-Ray Absorption Fine Structure. *Phys. Rev. Lett.* **1971**, *27*, 1204–1207.
- (40) International XAFS Society Error Reporting Recommendations: A Report of the Standards and Criteria Committee; http://ixs.iit.edu/subcommittee_reports/sc/err-rep.pdf (access Feb 2010).
- (41) Ravel, B.; Newville, M. ATHENA, ARTEMIS, HEPHAESTUS: Data Analysis for X-ray Absorption Spectroscopy using IFEFFIT. *J. Synchrotron Radiat.* **2005**, *12*, 537–541.
- (42) Diwald, O.; Sterrer, M.; Knözinger, E. Site Selective Hydroxylation of the MgO Surface. *Phys. Chem. Chem. Phys.* **2002**, *4*, 2811–2817.
- (43) Abel, E. W.; Butler, I. S. Halogenocarbonylmanganese Anions. *J. Chem. Soc.* **1964**, 434–437.
- (44) Parker, D. J. Infrared Spectra of bis[tetracarbonyl-(triphenoxyphosphine)-manganese]mercury and bis[tetracarbonyl-(tributylphosphine)manganese]mercury. *J. Chem. Soc. A* **1969**, 246–248.
- (45) Gibson, D. H.; Owens, K.; Mandal, S. K.; Sattich, W. E.; Franco, J. O. Synthesis and Thermolysis of Neutral Metal Formyl Complexes of Molybdenum, Tungsten, Manganese, and Rhenium. *Organometallics* **1989**, *8*, 498–505.
- (46) Almond, M. J.; Drew, M. G. B.; Sarikahya, F.; Senturk, O. S. Photochemical Synthesis and Crystal Structure of Dimethylphosphinodithiomanganese(I) Tetracarbonyl, $[\text{Mn}(\text{CO})_4(\text{S}_2\text{PMe}_2)]$. *Polyhedron* **1995**, *14*, 1433–1437.
- (47) Hartman, F. A.; Wojcicki, A. 0,0'-Dimethyldithiophosphate as a Monodentate Ligand. *Inorg. Nucl. Chem. Lett.* **1966**, *2*, 303–307.
- (48) Martin, T. A.; Ellul, C. E.; Mahon, M. F.; Warren, M. E.; Allan, D.; Whittlesey, M. K. Neutral and Cationic Mono- and Bis-N-heterocyclic Carbene Complexes Derived From Manganese and Rhenium Carbonyl Precursors. *Organometallics* **2011**, *30*, 2200–2211.
- (49) Butler, I. S.; Gilson, D. F. R.; Lafleur, D. Infrared Photoacoustic Spectra of Gaseous Pentacarbonyl(methyl)manganese(I) and Pentacarbonyl(methyl)rhenium(I). *Appl. Spectrosc.* **1992**, *46*, 1605–1607.
- (50) Elschenbroich, C. *Organometallics*, 3rd ed.; Wiley-VCH: Weinheim, Germany, 2006.
- (51) Little, B. J.; Wanniarachchi, S.; Lindeman, S. V.; Gardinier, J. R. Tricarbonylrhenium(I) and manganese(I) complexes of 2-(pyrazolyl)-4-toluidine. *J. Organomet. Chem.* **2010**, *695*, 53–61.
- (52) Pribula, C. D.; Brown, T. L. Metal-ion interactions with $\text{Mn}(\text{CO})_5^-$ in ether solutions. *J. Organomet. Chem.* **1974**, *71*, 415–425.
- (53) Morales, F.; Grandjean, D.; Mens, A.; de Groot, F. M. F.; Weckhuysen, B. M. Ray Absorption Spectroscopy of Mn/Co/TiO₂ Fischer–Tropsch Catalysts: Relationships between Preparation Method, Molecular Structure, and Catalyst Performance. *J. Phys. Chem. B* **2006**, *110*, 8626–8639.
- (54) Kim, K. J.; Park, Y. R. Optical Investigation of Charge-transfer Transitions in Spinel Co₃O₄. *Solid State Commun.* **2003**, *127*, 25–28.
- (55) Lu, J.; Serna, P.; Gates, B. C. Zeolite- and MgO-Supported Molecular Iridium Complexes: Support and Ligand Effects in Catalysis of Ethene Hydrogenation and H-D Exchange in the Conversion of H₂ + D₂. *ACS Catal.* **2011**, *1*, 1549–1561.
- (56) Uzun, A.; Ortalan, V.; Hao, Y.; Browning, N. D.; Gates, B. C. Imaging Gold Atoms in Site-Isolated MgO-Supported Mononuclear Gold Complexes. *J. Phys. Chem. C* **2009**, *113*, 16847–16849.
- (57) Campos, A.; Lohitharn, N.; Roy, A.; Lotero, E.; Goodwin, J. G.; Spivey, J. J. An Activity and XANES Study of Mn-promoted, Fe-based Fischer–Tropsch Catalysts. *Appl. Catal., A* **2010**, *375*, 12–16.
- (58) Stueben, B. L.; Cantrelle, B.; Sneddon, J.; Beck, J. N. Manganese K-edge XANES Studies of Mn Speciation in Lac des Allemands as a Function of Depth. *Microchem. J.* **2004**, *76*, 113–120.
- (59) Ramallo-López, J. M.; Lede, E. J.; Requejo, F. G.; Rodriguez, J. A.; Kim, J. Y.; Salas, R. R.; Domínguez, J. M. XANES Characterization of Extremely Nanosized Metal-Carbonyl Subspecies (Me = Cr, Mn, Fe, and Co) Confined into the Mesopores of MCM-41 Materials. *J. Phys. Chem. B* **2004**, *108*, 20005.
- (60) Housecroft, C. E.; Sharpe, A. G. *Inorganic Chemistry*; Pearson Education: New York, 2008.
- (61) Hadjiivanov, K. I.; Vayssilov, G. N. Characterization of Oxide Surfaces and Zeolites by Carbon Monoxide as an IR Probe Molecule. *Adv. Catal.* **2002**, *47*, 307–511.
- (62) Becker, J.; Wentrup, C.; Katz, E.; Zeller, K. P. Azulene-Naphthalene Rearrangement. Involvement of 1-Phenylbuten-3-yne and 4-Phenyl-1,3-butadienyldiene. *J. Am. Chem. Soc.* **1980**, *102*, 5110–5112.